Industrial Furnace Performance Under Carbon Capture Operation

P.M. Hughes, O. Ramadan, C. Lam, P. Gogolek, J. Wong, R. Lacelle, R. Lycett,

CanmetENERGY, Natural Resources Canada, 1 Haanel Drive, Ottawa, Ontario, Canada K1A 1M1

Abstract

Industrial combustion processes can represent as much as 30% of the CO_2 emissions from all combustion sources. One method to mitigate these emissions is to employ carbon capture and storage (CCS) technologies which involve the removal of the CO_2 from the exhaust gases. There is a large body of knowledge on the application of this technology to power boiler exhaust streams; however, there is much less information on the implementation to industrial processes. CCS technologies become more efficient as the concentration of CO_2 in the exhaust gas stream is increased. To concentrate the amount of CO_2 in the furnace, CCS combustion technologies recycle the exhaust gas stream, mix it with oxygen and feed this gas mixture back through the burner as a comburent. In this way, a concentration of over 90% CO_2 (mass basis) can be found in the exhaust. Over 80% of the exhaust products are recycled to the burners and the remaining 20% is sent to the carbon capture equipment. Under these operating conditions, it is not clear what the effects will be on the performance of the industrial process. This paper describes experiments undertaken with pilot-scale burners to compare the flame performance using air and CO_2-O_2 as a comburent with natural gas. In these experiments the nitrogen in the air is replaced by CO_2, keeping the O_2 in the comburent constant. The radiative, heat transfer and composition properties of the flames from three burners are compared for air and CO_2-O_2 as a comburent.

Corresponding Author:
Pat Hughes
Natural Resources Canada
CANMET Energy Technology Centre
1 Haanel Dr.
Nepean, Ontario
Canada
Email: phughes@nrcan.gc.ca
Tel: + 613-996-0827
Fax: +613-992-9335

Introduction

One method to mitigate CO_2 emissions from combustion processes is to employ carbon capture and storage (CCS) technologies which involve the removal of the CO_2 from the exhaust gases. CCS technologies become more efficient as the concentration of CO_2 in the exhaust gas stream is increased. To concentrate the amount of CO_2 in the furnace, CCS combustion technologies recycle the exhaust gas stream, mix it with oxygen and feed this gas mixture back through the burner as a comburent. In this way, a concentration of over 90% CO_2 (mass basis) can be found in the exhaust. The portion that is not recycled to the burner can be compressed and disposed of. In this way the CO_2 emissions from the combustion process can be significantly reduced. There is a large body of knowledge on the application of this technology to power boiler exhaust streams; however, there is much less information on the implementation to industrial processes. Questions such as how much exhaust to recycle and the effect of the comburent on the burner, flame and furnace performance must be answered.

There are many tools that can be used to establish the performance of an industrial furnace for particular combustion processes [1]. These tools can include references materials, pilot-scale testing with scaling rules and computational fluid dynamic modelling. Furnace and burner manufacturers use their own proprietary models to design equipment to suit specific combustion processes. The greatest success has been with air breathing natural gas combustion. Attempts have been made to include the influence of different fuels and oxygen enrichment with varying levels of success. The Scaling 400 series of tests [2] involved the study of a particular burner design covering the scaling range from 30 kW up to 12 MW. The focus of this research was to understand how NO_x formation in air breathing, natural gas combustion would scale up. Many models were developed [3] to predict the thermal NO_x formation in many different kinds of flames within the range of the scales tested. Many of the new burner technologies depend on the control of the mixing of the fuel and comburent and as such the CFD modelling has been less successful at scaling up the flame performance. Using the results of tests such as the scaling 400 program has been more successful at developing scale-up rules.

Before adopting the CCS technology for an industrial process it is necessary to establish the performance of flames operating in a high CO_2 environment. As such a series of tests were designed to operate three burners with air and a mixture of CO_2 and O_2 as comburents. A variety of measurements were made to determine the effect of CO_2 on the flame and furnace performance. This paper discusses some of the results of these experiments.

Tests to be Performed

As part of the test program to study the performance of industrial burners and furnaces under CCS conditions, two commercial burners and one research burner were chosen to operate in the pilot-scale Research Tunnel Furnace Facility at the CanmetENERGY laboratories. The test conditions were chosen such that the burners would operate at 200 kW using natural gas as the fuel and the comburent would be either air or a combination of CO_2 and oxygen. The mass flow rate of oxygen (either from the air or from the CO_2 - O_2 mixture) was fixed at about 60.5 kg/h. This corresponds to an air flow rate of about 261 kg/h. The CO_2 flow rate (approximately 303 kg/h) was chosen to approximately simulate the volume flow rate of nitrogen if air were flowing. The reason for this choice

was to ensure that the near burner aerodynamic properties were nearly constant. This would allow the study the effect of the flame and furnace performance by simply exchanging nitrogen for CO_2. The test conditions are given in Table 1.
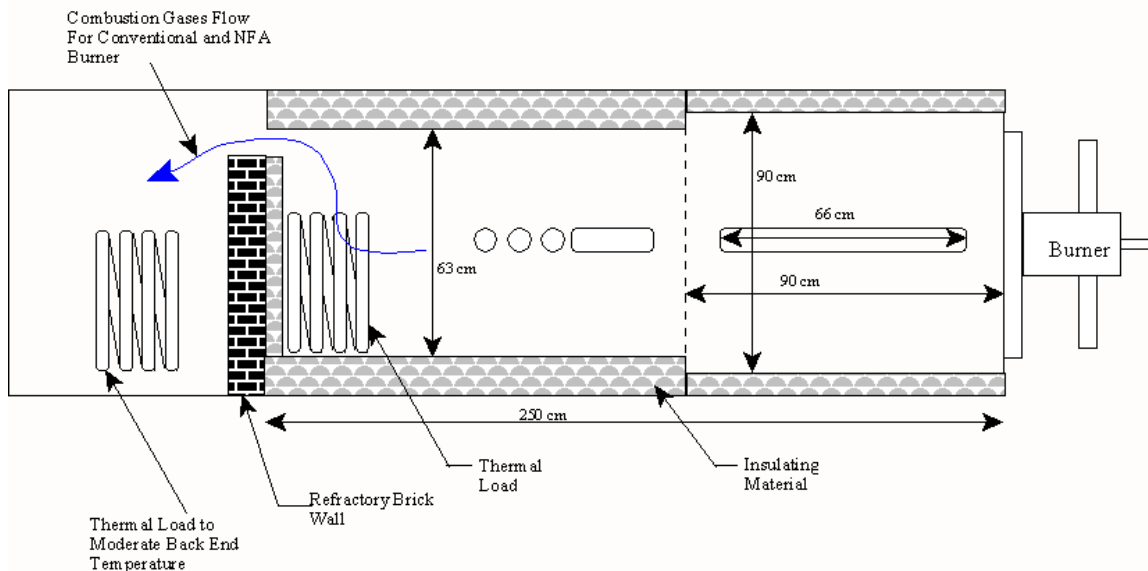
Table 1: Test Conditions

Comburent	Air (kg/h)	Oxygen (kg/h)	CO_2 (kg/h)	Natural Gas (kg/h)
Air	261			13.8
CO_2 - O_2	-	60.5	303	13.8

Test Furnace

The Research Tunnel Furnace (RTF) is shown in Figures 1 and 2. The RTF is cylindrical in shape and the burners are mounted on the end and the flame and combustion gases are made to flow along the central axis. Provision is made to probe the flame through ports in the side wall of the furnace. Figure 3 shows the interior of the RTF. The first 90 cm of the furnace is 90 cm in diameter. The remaining 160 cm have a diameter of 63 cm. A wall made of refractory brick and blanket insulation is located at 250 cm from the burner to form an enclosure to simulate the high temperature conditions in a full-scale industrial furnace. A cooling coil (Fig. 1 and 3) is located just before the wall to simulate a thermal load on the furnace gases. A measurement of the coolant flow rate and the temperature rise enabled the calculation of the heat picked up by this thermal load.

Figure 1: Schematic of the interior of the Research Tunnel Furnace.
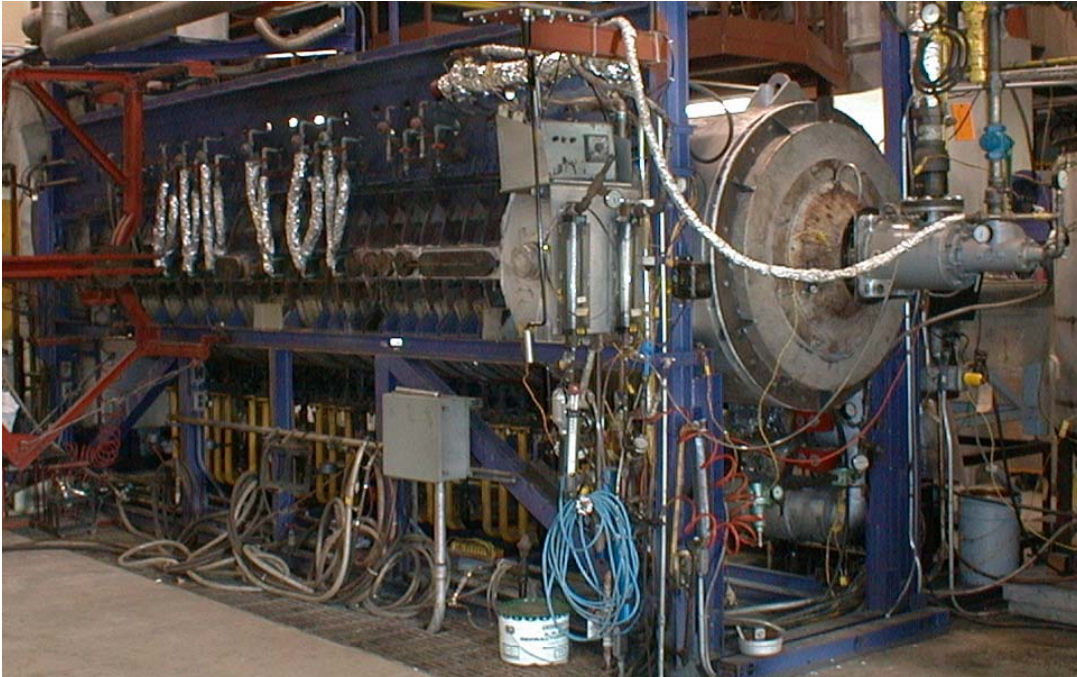
Figure 2: Photograph of the RTF.

Figure 3: The inside of the RTF showing the insulation and the heat transfer coil just before the wall.

Burners Tested

The three burners used in the tests are shown in Figures 4, 5 and 6. The commercial Low NO_x burner in Fig. 4 has the comburent flow through the 4 rectangular ports around the central fuel pipe. This burner was chosen to represent the majority of burners in use in industry. This burner could be used in recuperated or non-recuperated combustion systems. No recuperation was simulated for these tests.
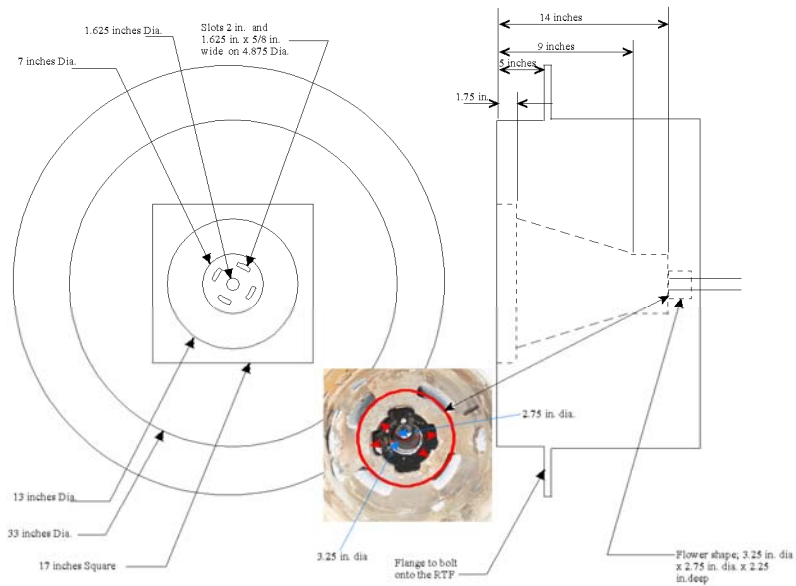
Figure 4: Commercial Low NO$_x$ burner.
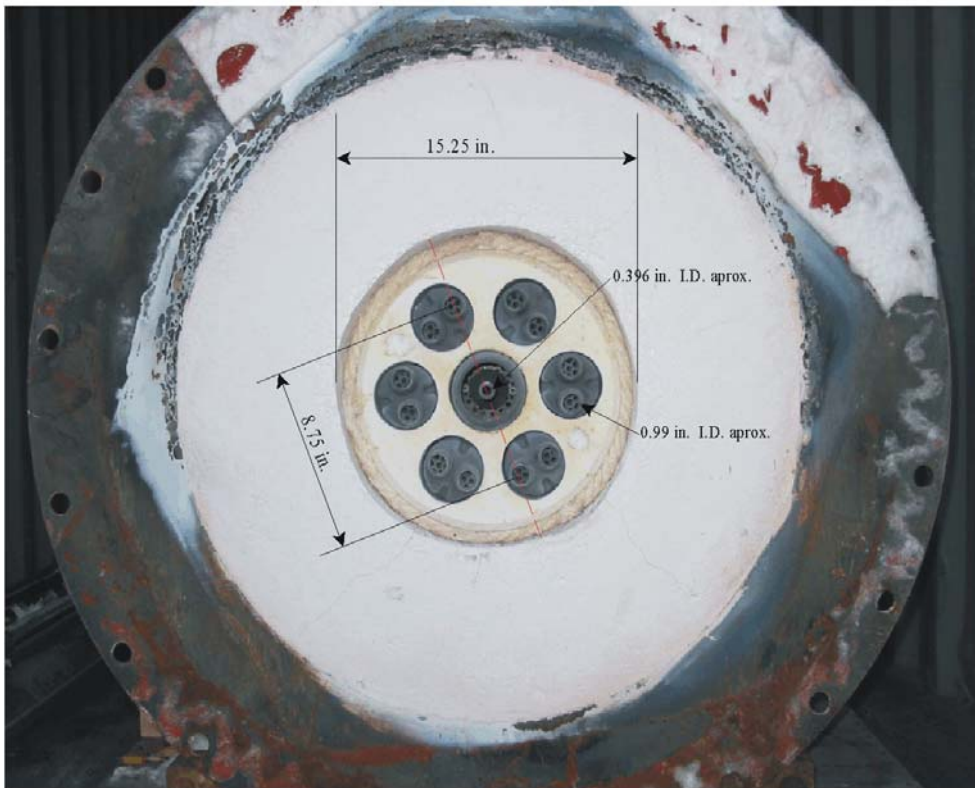
Figure 5: Commercial regenerative burner.

The regenerative burner shown in Fig. 5 was chosen to represent a class of advanced burners, some of which are being used in industrial furnaces. This is a self regenerated burner where the comburent enters through three of the six entry ports around the central fuel pipe. The comburent picks up heat from regenerative material in the entry ports. At the same time furnace gases are drawn out through the remaining three ports thereby heating up the regenerative material in these ports. This flow pattern occurs for about 10 seconds and then the entry and exit ports are switched and in so doing the regenerative material is kept at a high temperature. As well the comburent is heated to a very high temperature and the gases leaving the furnace through the burner are cooled to about 150 C.

The IFRF Near Field Aerodynamics (IFRF-NFA) burner is shown in Fig. 6. The IFRF moving block swirl generator was attached to this burner so that the comburent was given a swirl component. This is the same combination that was used in the Scaling 400 tests. The natural gas entered the swirling flow through the small holes at the end of the gas gun shown in the figure. The gas gun was placed at the zero position and the estimated swirl number of the air flow is 0.5. The swirling air and fuel enter the furnace through the 132 mm diameter port in the burner.
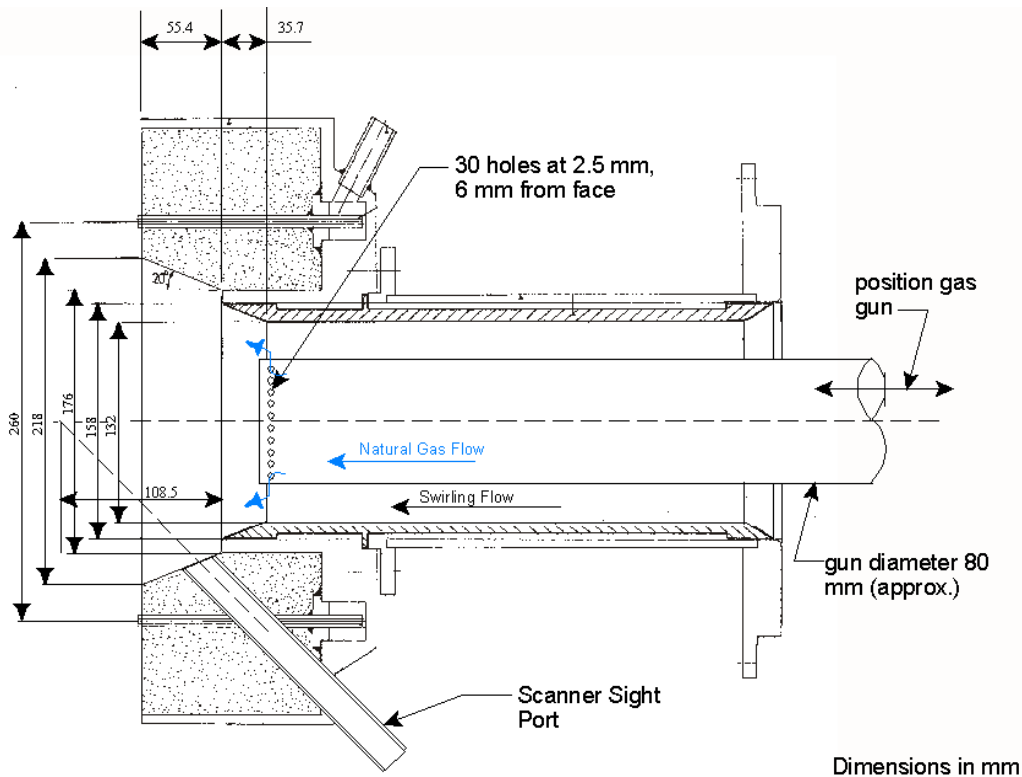
Figure 6: IFRF Near Field Aerodynamics (IFRF-NFA) burner.

Measurement Techniques
Inserted Probe Measurements
Gas temperature and composition were measured using water cooled probes. The gas composition probe uses convective cooling to quench the sampled gas. The gas temperature is measured using a suction pyrometer.

Narrow Angle and 2 pi Radiometers
Radiance measurements were made in the furnace using a narrow angle radiometer (NAR). The NAR was designed at the International Flame Research Foundation [4, 5]. This probe was used in previous measurements in similar burners at the Canmet/ENERGY laboratories; however, for the tests reported here, the thermistor detector was replaced by a thermopile. This gave stable, more reliable radiance measurements.

Incident radiance flux measurements were made using a two pi radiometer [6]. The functioning of this probe is described in the IFRF handbook [7].

The orientation of these two radiometers is shown in Figure 7. With the cold target in place, the NAR measures the flame radiance and is used to estimate the flame emissivity. With the furnace brick placed opposite the NAR probe it is possible to measure the radiance from the wall as well.
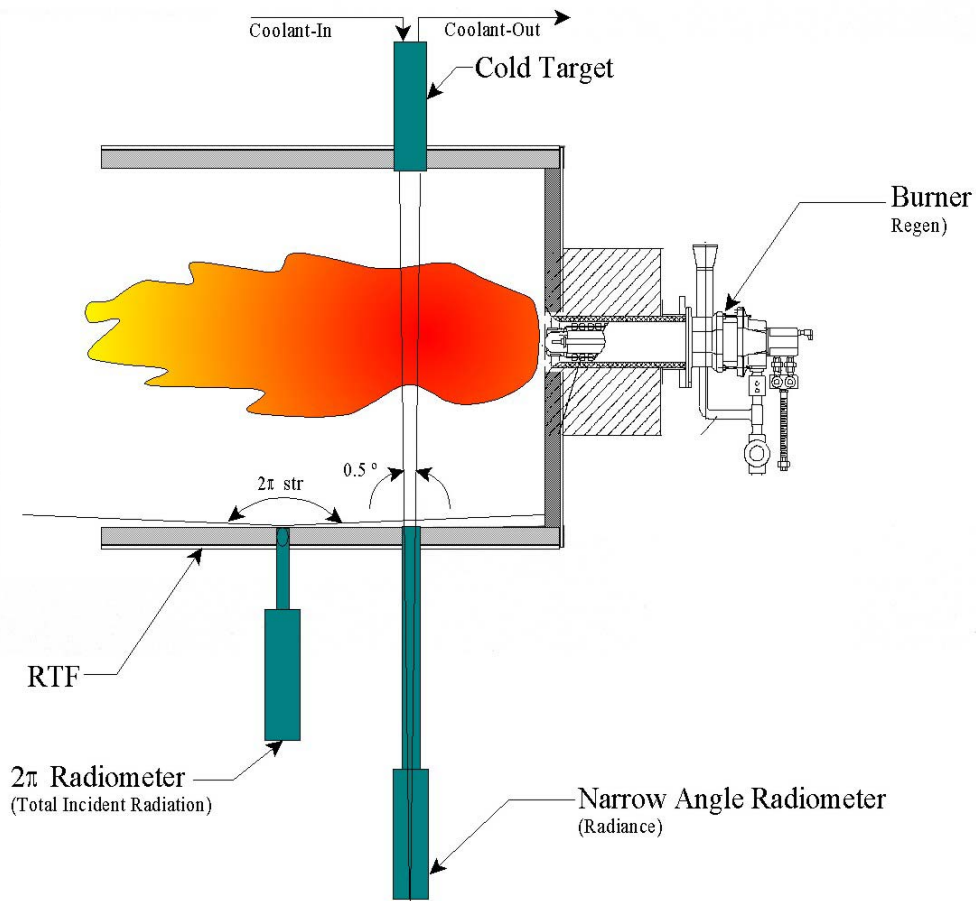
Figure 7: Narrow angle radiometer and 2 pi radiometer measurements in the research furnace.

Total Heat Flux

The total heat flux from the flame and furnace walls was measured with a device that was fabricated in the Canmet/ENERGY facilities and based on the design by Keltner et al. [8]. A schematic of the total heat flux probe is shown in Figure 8. Additional details of the probe are provided in Lam et al. [9]. The probe was placed in the same orientation as the 2 pi radiometer in Fig. 7.
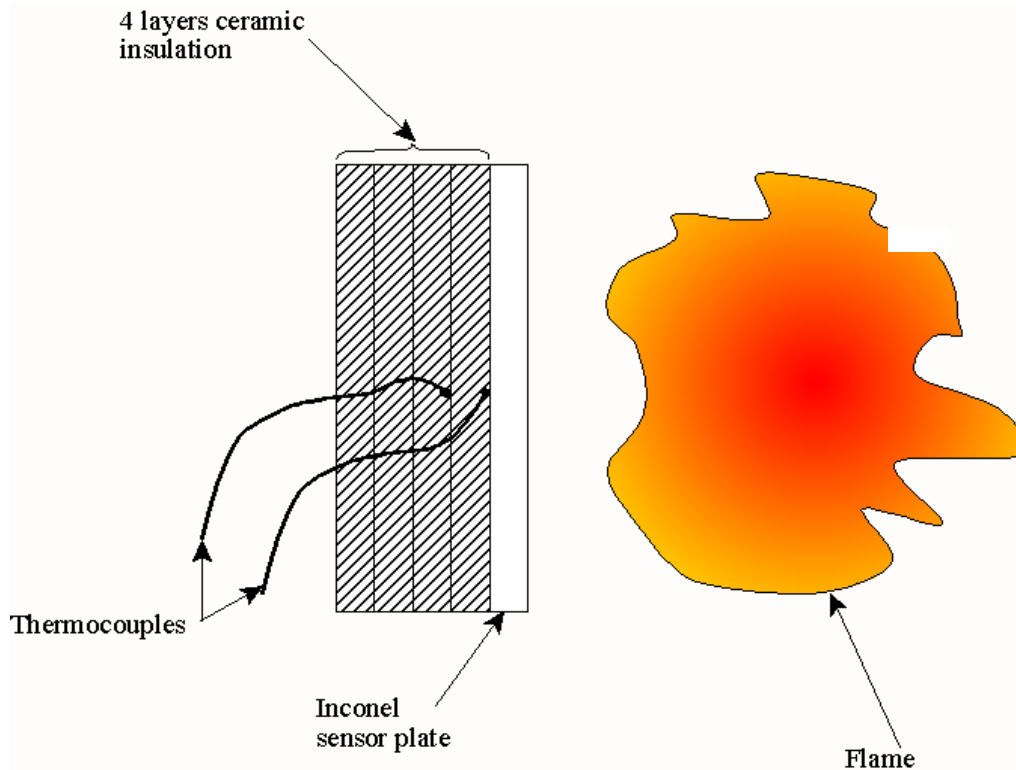
Figure 8: Schematic of the Total Heat Flux Probe.

IR Camera
A Merlin Mid IR camera from FLIR was used to capture infrared images through the side ports. A CO_2 filter was used to eliminate the radiance from the flame so that the camera captures only the radiation from the far wall.

Results:
Combustion Chamber Temperature

The temperature of the combustion chamber was monitored with a thermocouple (in a ceramic shield) mounted in the wall of the furnace about 25 cm from the burner face. Table 2 shows the chamber temperature measurement for all six tests. As can be seen in this table the replacement of the nitrogen by CO_2 in the comburent has the effect of reducing the average chamber temperature. This is most likely due to the difference in the specific heat between nitrogen and CO_2.

Table 2: Average Chamber Temperature (C)

Burner	Air Operation	CO_2-O_2 Operation	Difference
Low-NO$_x$	1026	996	31
IFRF-NFA	1068	999	69
Regenerative	1138	1075	63

It is interesting to note that the difference in the chamber temperature for the two operating conditions varies with the burner type used. As will be seen later this same trend is found for the average wall temperature, measured using an IR Camera in the near burner region. This trend may be due to the different flow fields in the near burner region

of the burners resulting in differing convective interactions between the furnace gases and the walls of the furnace.

Regenerator Temperature

The gas temperature in the regenerator was measured just as the gas was leaving the regenerator (stack end) and entering the furnace (furnace end). Typical regenerator measurements are shown in Figures 9 and 10.
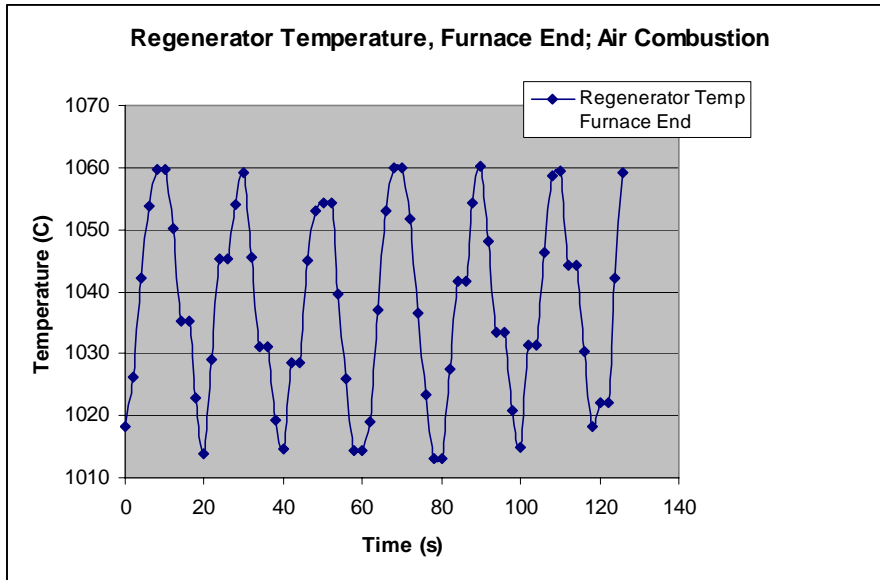

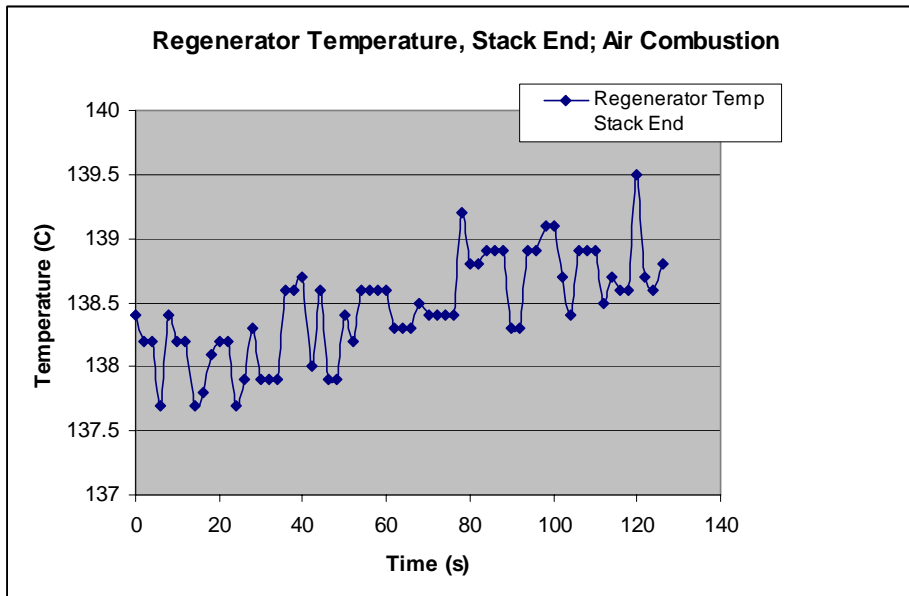**Figure 9: Typical gas temperature measured in the regenerator at the furnace end.**

Figure 10: Typical gas temperature measured in the regenerator at the stack end.

As can be seen the temperature varied over the complete cycle of the burner operation at both the furnace and stack ends. Table 3 shows average values of the gas temperature at the furnace and stack end of the regenerator as measured during many 8 hour tests with the regenerative burner for both air and CO_2-O_2 operation.

An estimation of the furnace end gas temperature in the regenerator for CO_2-O_2 operation using the temperature for air operation and the specific heats of the different comburents is 937 ^{o}C. This is rather close to the measured temperature of 986 ^{o}C but a better estimate could be made if the heat loss in the burner were accurately known.

Table 3: Average Regenerator Gas Temperature (C)

Location in Regenerator	Air	CO_2-O_2	Difference
Furnace	1073	986	87
Stack	140	139	1

CO Composition and Gas Temperature

Figure 11 shows the distribution of the CO in the furnace for the three burners and for the two operating conditions. As can be seen the CO is consumed at a faster rate for the CO_2-O_2 combustion conditions for the three burner configurations. That is to say the region of high CO concentration is larger for the air combustion than that for the CO_2-O_2 comburent. The combustion in the regenerative burner occurs far from the burner but the high CO region is still shown to be smaller for the CO_2-O_2 operating conditions.

The relationship between the centre line gas temperature and the corresponding CO concentration is shown in Figure 12. The Low NOx and the regenerative burner graphs show that the faster reactions in the CO2-O2 flames result in an early high gas temperature. Possibly the measurements in the IFRF-NFA burner were not made close enough to the burner to show this phenomenon.
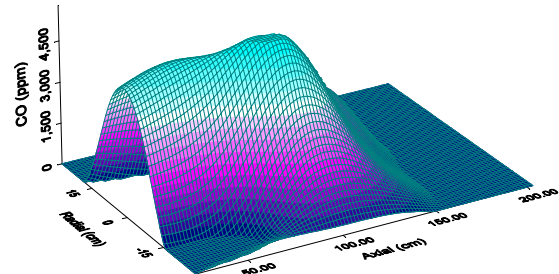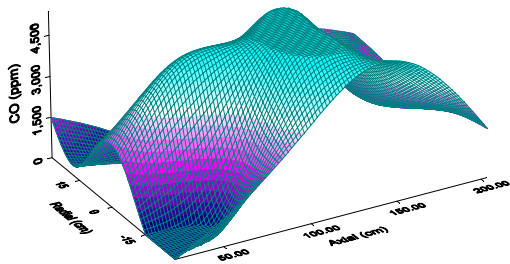
Air   CO$_2$-O$_2$
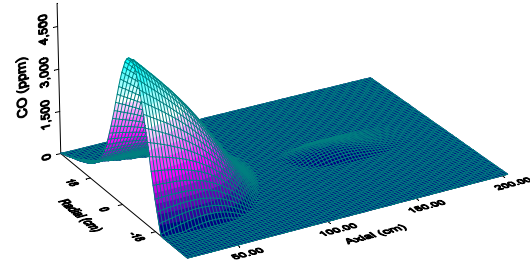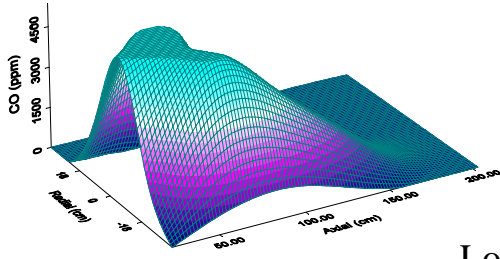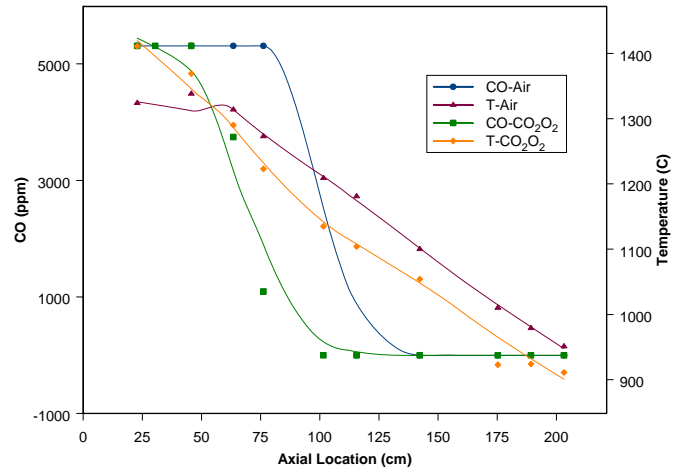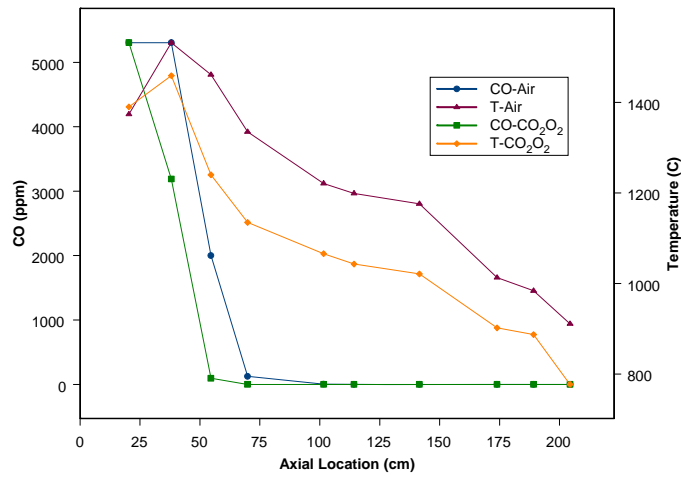
Low NO$_X$
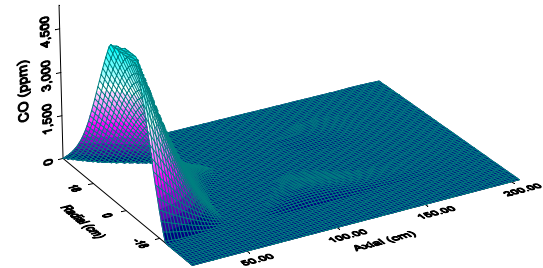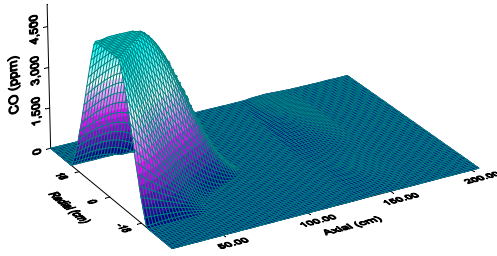
IFRF-NFA

Regenerative

Figure 11: Carbon Monoxide Surface in the Near Burner Region for the Three Burners and the Two Combustion Conditions.

Low NO$_x$ Burner; Centre Line Measurements

IFRF-NFA Burner; Center Line Measurements
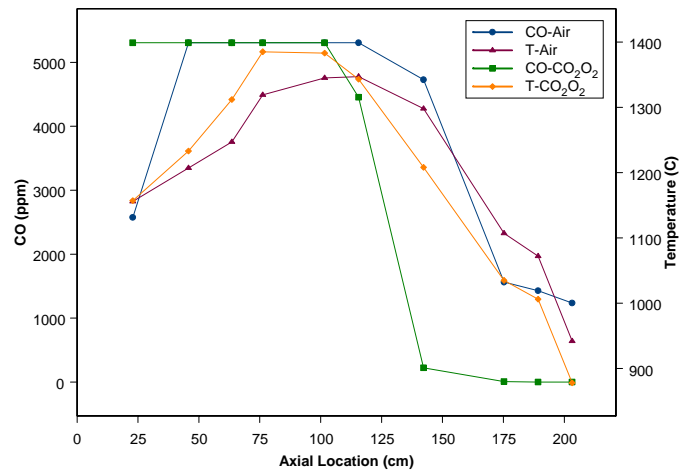
Regenerative Burner; Center Line Measurements

Figure 12: Axial variation of the center line CO and gas temperature for the three burners and the two operating conditions

Measurements with the Narrow Angle Radiometer

The Narrow Angle Radiometer (NAR) measurements were only done in the IFRF-NFA burner. Figures 13 and 14 show the radiance and emissivity measurements for the air and CO_2-O_2 operations. The NAR measurements in the Low NOx and regenerative burners have been reported in an earlier publication by the author [10].
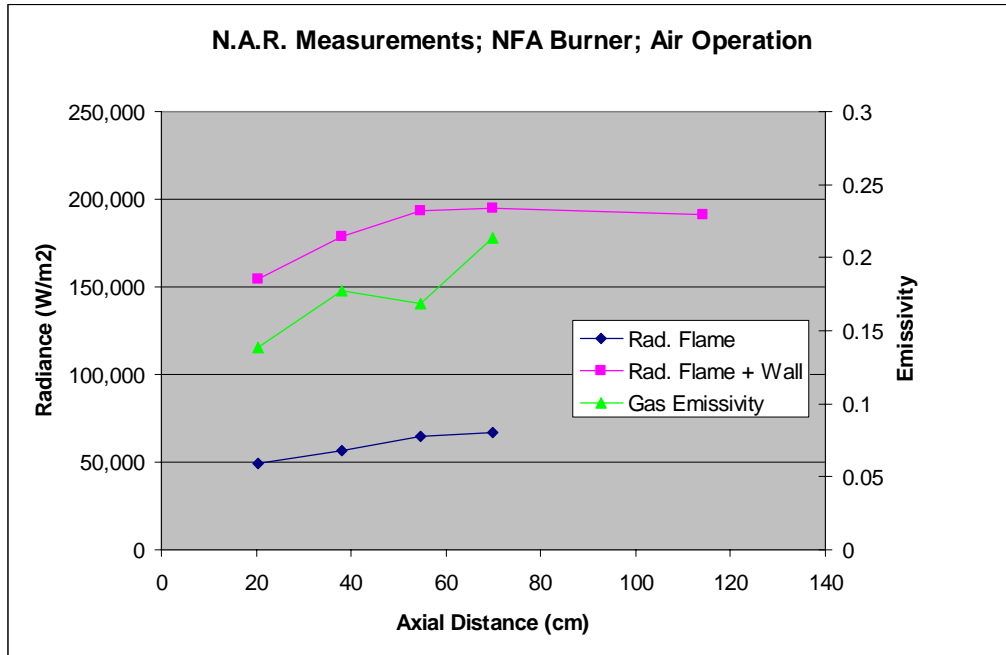

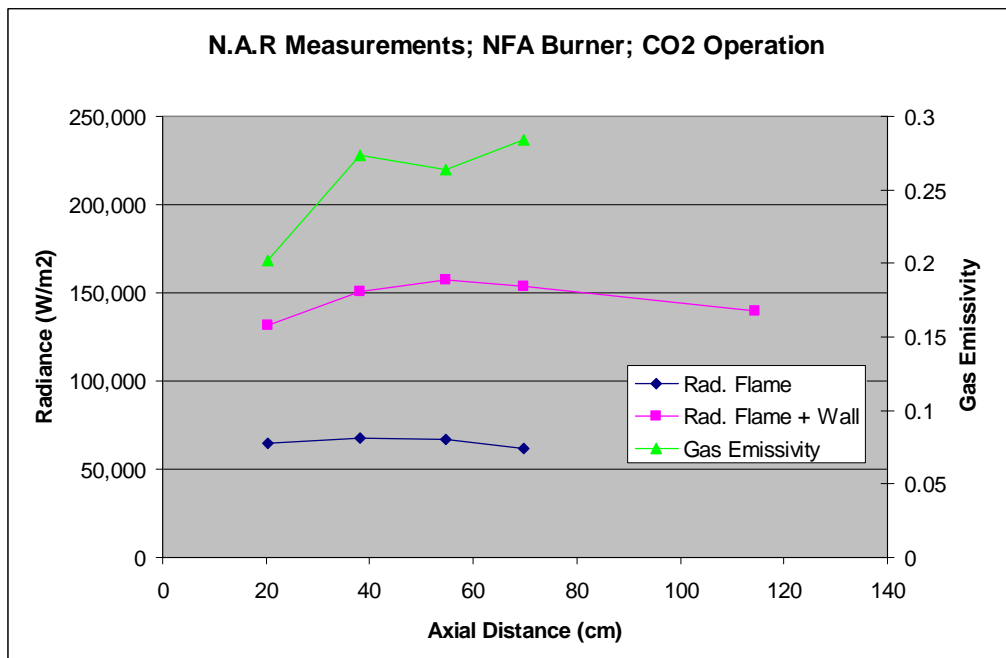**Figure 13: Radiance and emissivity measurements in the IFRF-NFA burner with air as comburent.**

Figure 14: Radiance and emissivity measurements in the IFRF-NFA burner with CO2-O2 as comburent.

For the CO_2-O_2 operation the flame alone is shown to have a slightly higher radiance than that for the air as comburent. This probably due to the initially higher CO_2-O_2 gas temperature discussed above. The flame radiance eventually falls below that of the air

combustion due to the reduced gas temperature in the CO_2-O_2 flame. Because of the higher wall temperature the total radiance (flame plus wall) is much higher in the air flame.

The flame emissivity is much higher in the CO_2-O_2 flame due to the increased CO_2 concentration. The measured emissivity in the air and CO2-O2 flames at the farthest location from the burner is shown in Table 4. The calculated values use the charts developed by Hottel et al [11].

Table 4: Measured and Calculated Flame Emissivities

Comburent	Measured	Calculated
Air	0.213	0.125
CO2-O2	0.284	0.20

The total radiance measurements (flame plus wall) are lower for the CO_2-O_2 flame. The higher flame emissivity in the CO_2-O_2 combustion does not make up for the lower flame and wall temperatures.

Heat Flux Measurements

Aside from the NAR measurements the various modes of heat transfer in the furnace were measured using a 2 pi radiometer (incident heat flux), a total heat flux probe, and an IR camera.

Total Heat Flux

The total heat flux was measure at port 3 and for only the IFRF-NFA burner. These results are shown compared to the 2 pi measurements in the same port in Table 5. The values for the convected heat transfer are calculated from the difference between the 2 pi (incident radiant flux) and the total heat flux. The convected heat transfer at the walls of the furnace has an average value of about 7% of the total heat flux for these tests.

Table 5: Comparison of the Total and Radiant Flux at Port 3 for the IFRF-NFA Burner

Comburent	2 pi (W/m^2)	Total (W/m^2)	Convected (W/m^2)
CO_2-O_2	138,432	148,724	10,292
CO_2-O_2	127,867	152,468	24,601
Air	180,561	181,646	1,085
Air	179,566	189,139	9,573

IR Camera: wall temperature and radiation

Wall Temperature
Figure 15 shows the layout of the inside wall of the furnace. This is the location of the IR images captured during the tests. The burner is located at the right end of the image in Fig. 15. The IR camera was used to measure the heat flux from the wall and the wall

temperature. Figure 16 shows a typical IR image captured during the tests and the line along which the wall temperature is measured. The shielded thermocouple used to measure the chamber temperature in the tests is also shown in these figures.
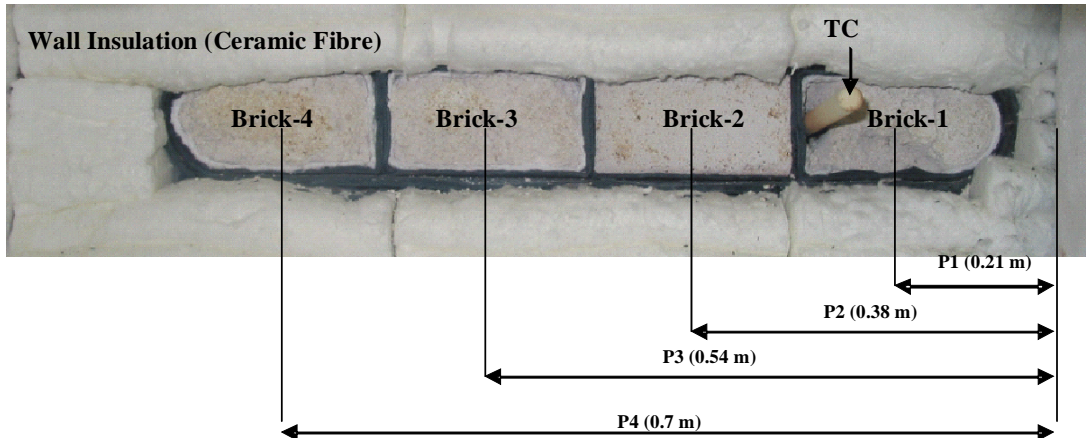

Figure 15: View of the inside of the test furnace "seen" by the IR camera.
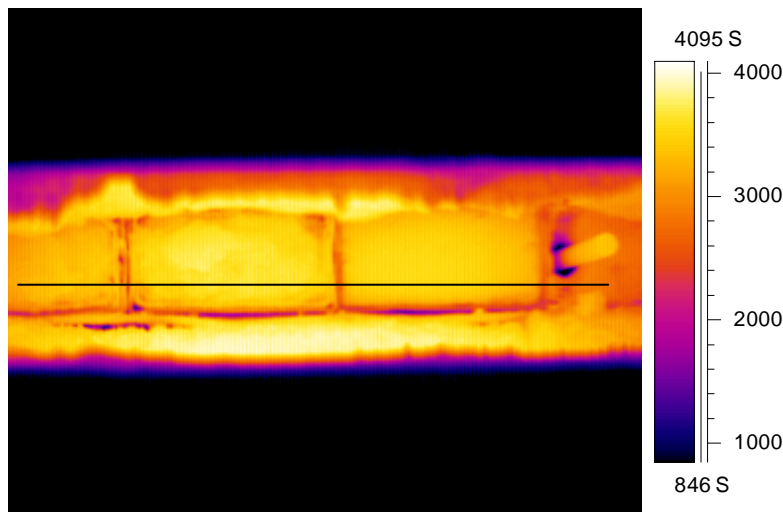

Figure 16: False colour IR image of the inside of the test furnace showing the line along which the wall temperature was measured.

Figures 17 to 19 show the wall temperature measured for the three burners and the two combustion conditions.
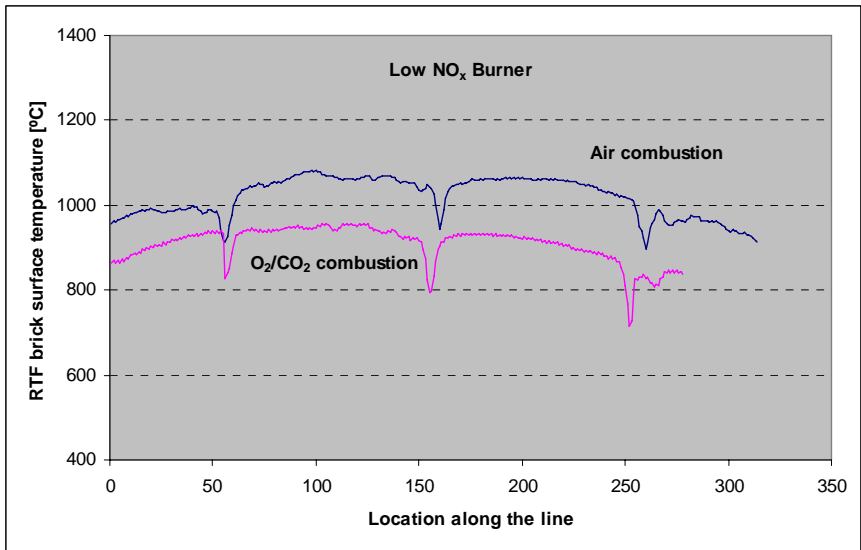
Figure 17: Wall temperature along the line shown in Fig. 15 for the Low NOₓ burner as measured using the IR camera image.
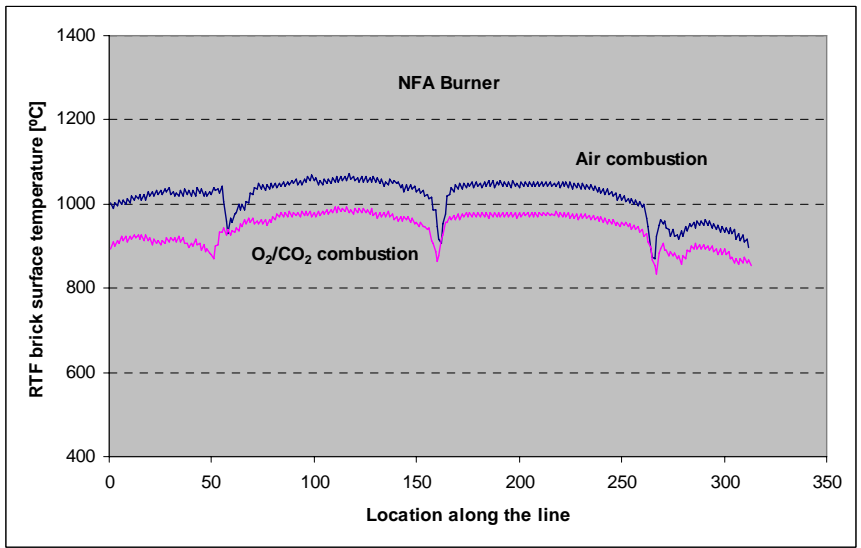

Figure 18: Wall temperature along the line shown in Fig. 15 for the IFRF-NFA burner as measured using the IR camera image.
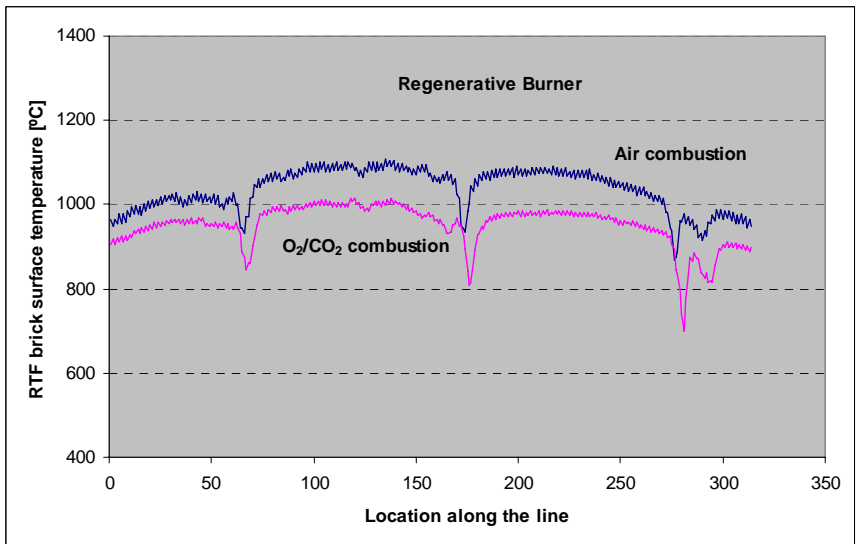

Figure 19: Wall temperature along the line shown in Fig. 15 for the regenerative burner as measured using the IR camera image.

Table 6 shows a comparison of the average and maximum wall temperatures measured along the lines shown in Figs. 17 to 19. The trends are similar to those measured for the chamber temperature (Table 2). The wall temperature is always lower for the CO_2-O_2 combustion compared to the air combustion. As well it appears as though the wall temperature is always lower than the chamber temperature for the CO_2-O_2 combustion.

Table 6: Typical Average and Maximum Wall Temperatures (^{o}C)

Burner		Air Operation	CO_2-O_2 Operation	Difference
Low-NO$_x$	Average	1028	920	108
	Maximum	1081	958	123
IFRF-NFA	Average	1028	950	78
	Maximum	1072	993	79
Regenerative	Average	1047	966	81
	Maximum	1108	1016	92

Wall Radiation

Figures 20 to 22 show the axial variation of the various heat fluxes measured in the furnace for the three burners tested and the two operating conditions. As discussed above the 2 pi radiometer measures the incident radiant flux to a point as viewed over 2 pi steradians. The IR camera measures the radiant flux directly from the wall towards the camera. The total heat flux probe measures the total heat flux incident on a plate at the wall. This plate views 2 pi steradians however the "view factor" changes as one moves away from the perpendicular. The NAR measurements shown here are those captured without the cold target and so include the contributions from the wall and the flame in the small 0.5 degree view angle.

The heat flux measurements are always higher in the air combustion flame. This is due to the higher gas and chamber temperatures in the air combustion. The 2 pi measurements are always higher than those made by the IR camera. This is due to the fact that the 2 pi radiometer includes more of the furnace in the field of view than does the IR camera. The 2 pi radiometer sees higher temperature regions of the furnace. The regenerative burner always has a higher radiative heat transfer compared to the other burners and is probably due to the even distribution of a high gas temperature.

The NAR measurements (in Fig 21) are shown to be higher than the other heat flux measurements for both of the operating conditions. This may be due to the small field of view (0.5 degrees) of the NAR probe. The IR camera measurements shown in Figs. 20 to 22 are calculated as averages over the individual bricks shown in Figs. 15 and 16. As can be seen in Fig.s 17 to 19 the signal capture by the IR camera varied significantly over the individual brick. It would be better to compare the maximum IR measurement to the NAR measurements. In the IFRF-NFA burner, the maximum radiation measured along the line shown in Fig. 16 by the IR camera for the air combustion is about 20.2 w/cm^2 and 12.5 W/ cm^2 for the CO_2-O_2 combustion. This compares much better with the NAR measurements.
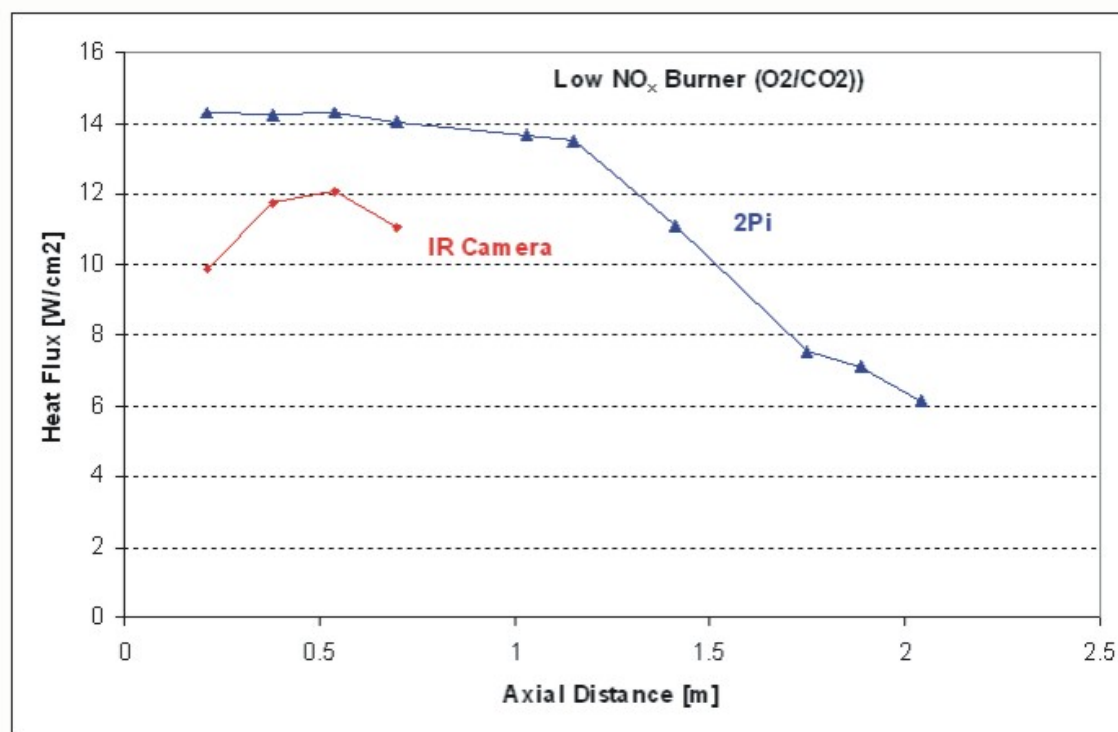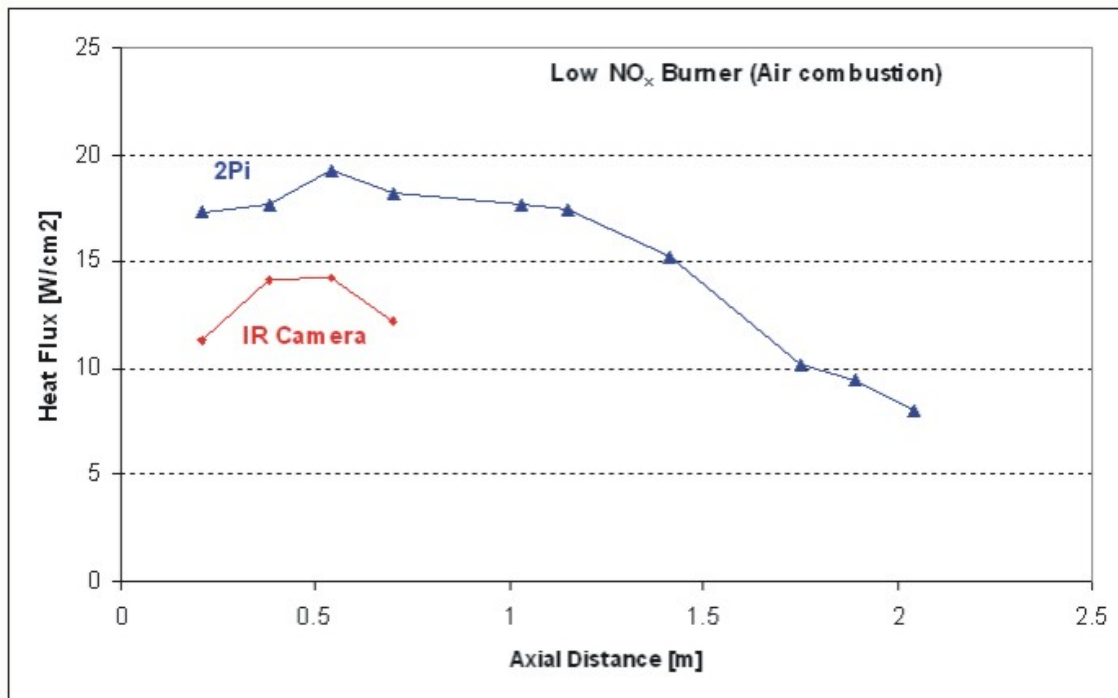
Figure 20: Axial variation of the measurements of the 2pi radiation and the wall heat flux for the Low NOx burner for the two operating conditions.
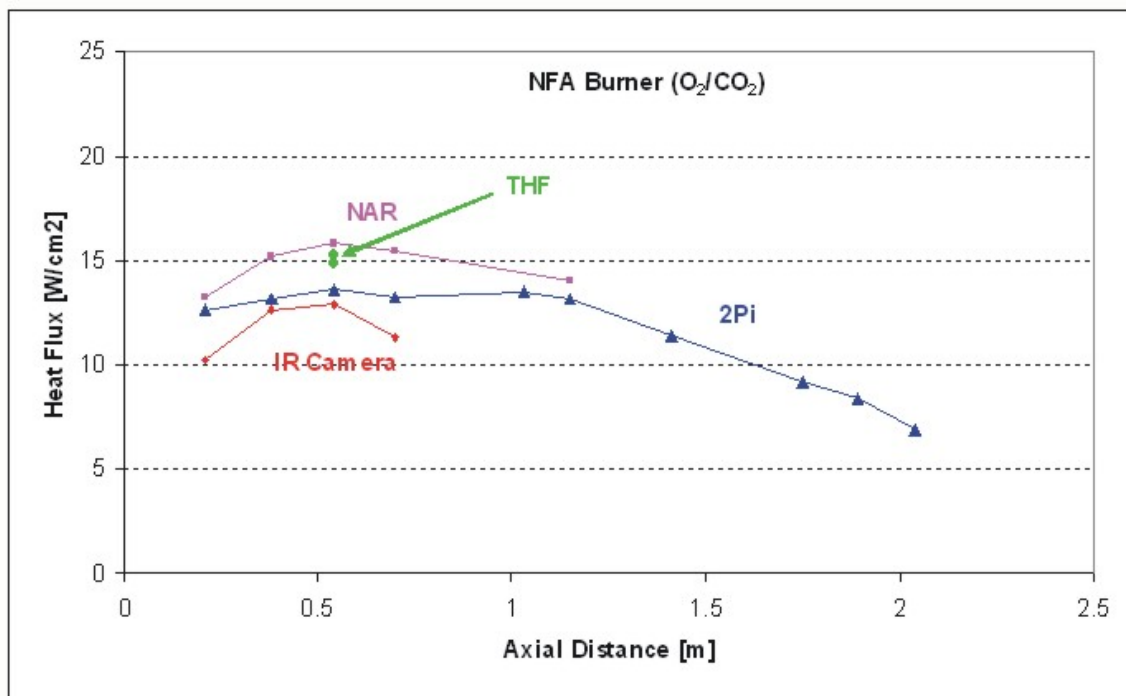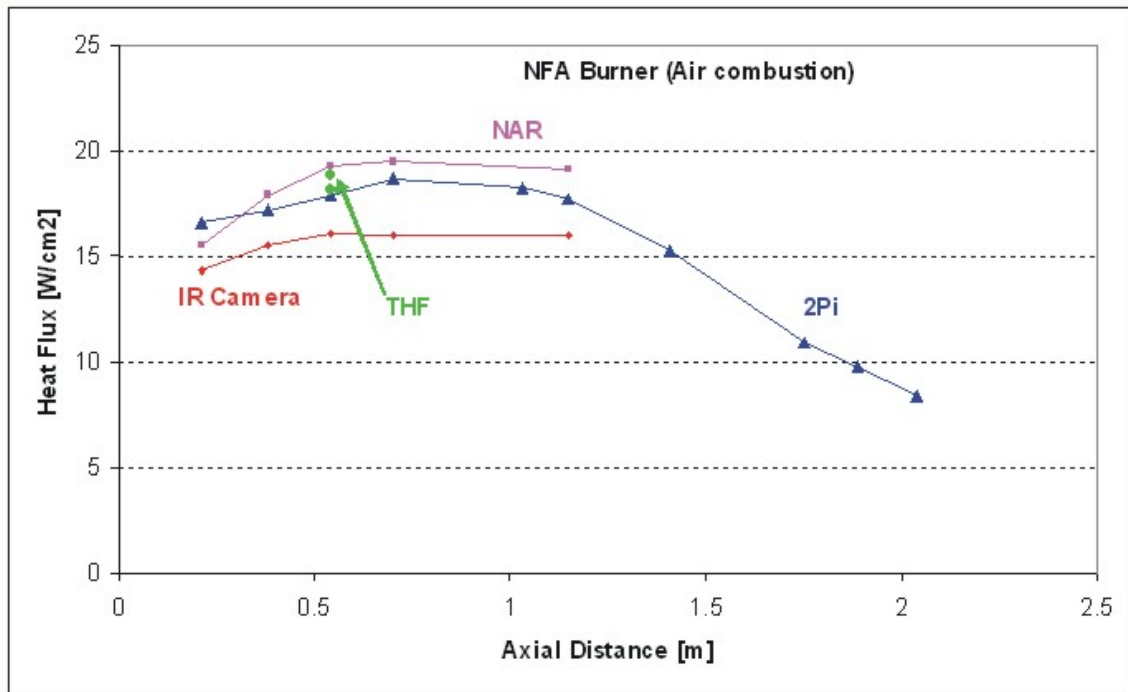
Figure 21: Axial variation of the measurements of the 2pi radiation, narrow angle radiation, total heat flux (THF) and the wall heat flux for the IFRF-NFA burner for the two operating conditions.
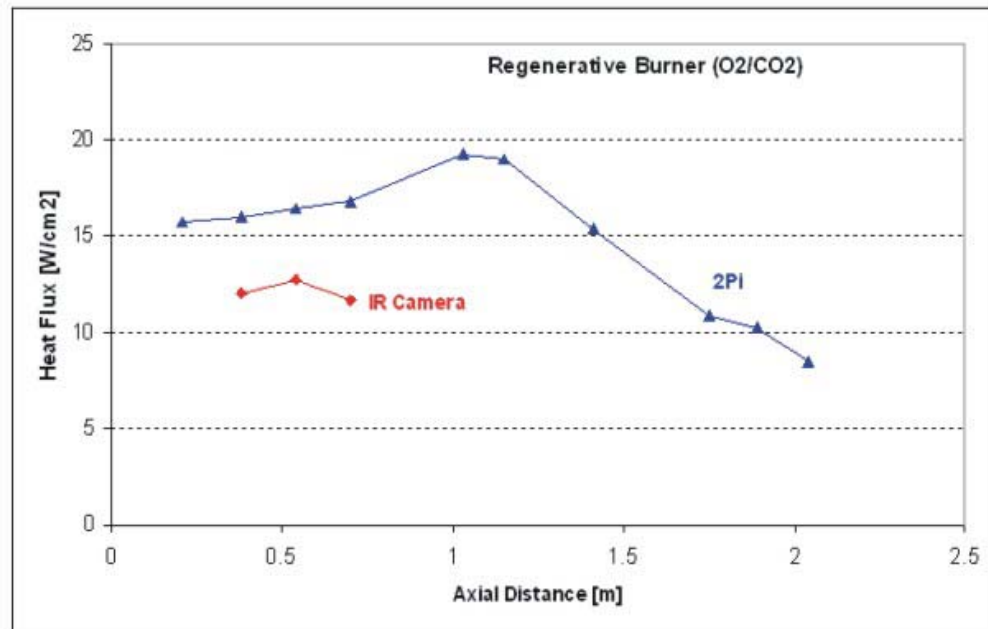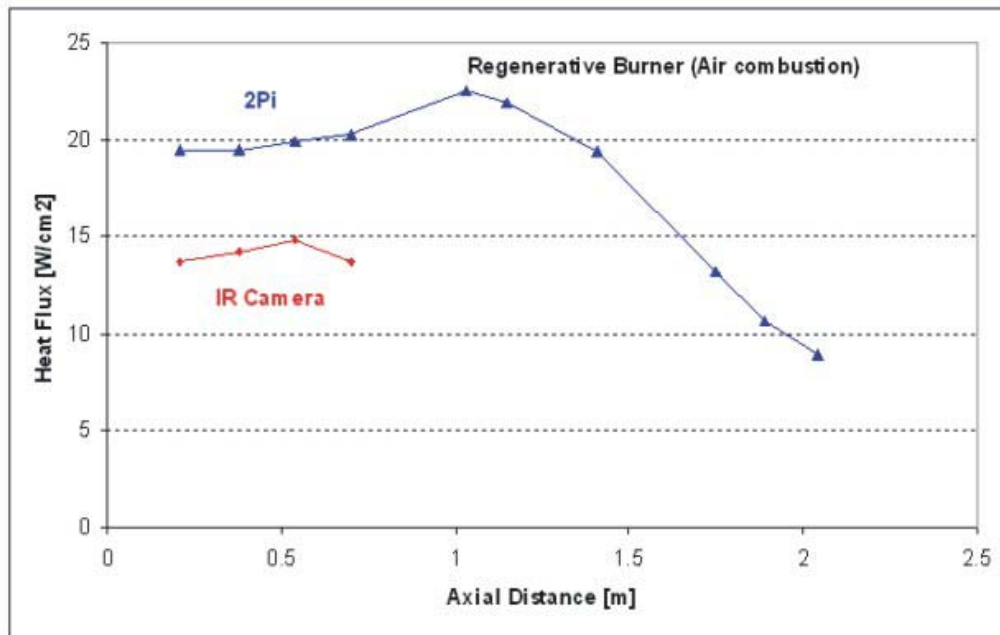
Figure 22: Axial variation of the measurements of the 2pi radiation and the wall heat flux for the regenerative burner for the two operating conditions.

Heat transferred to the load

Figure 23 shows the variation of the heat picked up by the coil just before the wall in the furnace. The combustion tests where the comburent was CO_2-O_2 are indicated with a red circle around the data point. As can be seen the tests with the Low NO_x burner had the widest variation in heat transfer. As well, for the most part the heat transfer is lower for the CO_2-O_2 comburent tests. The regenerative burner is shown to have the highest heat transferred to the load for all of the tests. The Low NO_x burner has the lowest heat transferred to the load.
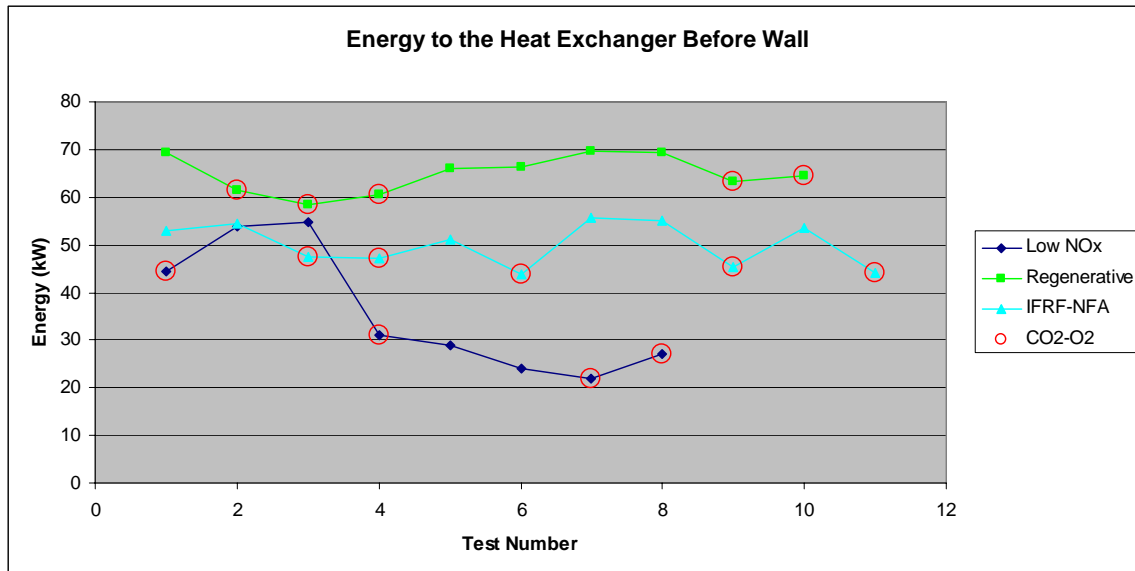
Figure 23: Heat transferred to the load in the furnace for the three burners and the two operating conditions.

Conclusions

Tests were conducted to compare the performance of burners operating under conditions simulating CCS operation with those with air breathing combustion.

The distribution of the CO in the CCS flames was found to be smaller than for the air breathing combustion.

As expected the gas and wall temperatures were found to be lower for the CCS conditions. The reason for this is due to the difference in the heat capacity for CO_2 compared to that for nitrogen.

The total emissivity of the CCS flame was measured and found to be higher than that for air breathing combustion.

Various forms of heat flux were measured in these flames using different measurement techniques. The heat fluxes were found to be consistent across the measurement techniques. The regenerative burner is shown to have a consistently higher radiated heat transfer than the other burners.

Of the three burners, the regenerative burner had the highest heat transferred to the load and had the smallest difference between the CCS and air breathing operating conditions.

Further tests need to be conducted to determine the optimum amount of exhaust gas to recirculate to minimize the temperature loss to the CO_2 and to explore the detailed effect on the combustion and aerodynamics in the near burner region. It will also be necessary to determine the effect of using different fuels and the performance in different combustion processes. The rules for scale up of these results will be investigated.

References

1. "North American Combustion Handbook, Volumes 1 and 2"; ISBN 0-9601596-3-0.
2. Weber, R. "Scaling charascteristics of aerodynamics, heat transfer, and pollutant emissions in industrial flames", Twenty-Sith Symposium (International) on Combustion/The Combustion Institute, 1996, pp. 3343-3354.
3. Hsieh, T. C. A., Dahm, W. J. A. and Driscoll, J. F., "Scaling laws for NOx emission performance of burners and furnaces from 30 kW to 12 MW", Combustion and Flame, volume 114, pp. 54-80, 1998.
4. Lallemant, N., Locquet, J. J., "Theory and Design of Narrow Angle Radiometer Probes", IFRF document No. C73/y/1, 1998.
5. Fricker, N., "How do I measure radiation with a Narrow Angle Radiometer?", IFRF Online Combustion Handbook, IFRF Doc. No. C76/y/1/9, 2001.
6. Holthuysen, A., M., "Ellipsoidal radiometer", IFRF Doc. No. C76/y/1/3, 1994.
7. Fricker, N., "How do I measure thermal radiation with an ellipsoidal radiometer?", IFRF Online Combustion Handbook, IFRF Doc. No. C76/y/1/3, 2001.
8. N.R. Keltner, J.V. Beck and J.T. Nakos, "Using Directional Flame Thermometers for Measuring Thermal Exposure", Journal of ASTM International, 7(2), 2010.
9. C.S. Lam , O. Ramadan, J. Wong, R. Lycett and P.M. Hughes, "Heat Flux Measurement in Industrial Furnaces", Proceedings of 2010 Spring Technical Meeting, Combustion Institute - Canadian Section, Ottawa, Ontario, May 9-12, 2010, pp. 415-420.
10. P. M. Hughes, R. J. Lacelle, A. Idris, M. Legere, D. Percy, J. Wong, T. Parameswaran, "CARS and Heat Flux Measurements in Regenerative and Conventional Industrial-Scale Burners", IFRF Online Industrial Journal, Article No. 200901, March 2009.
11. Hottel, H. C. and Egbert, R. B., "Radiation Heat Transfer From Water Vapor" AIChE Trans., Vol. 38, 1942.